


Research Article

Synovial-Derived Mesenchymal Stem Cells Encapsulated in Alginate Beads Provide Better Outcomes for Equine Tarsus Chondral Lesions

Vitor Hugo Santos^{1,2}, João Pedro Hübbe Pfeifer², Gustavo Santos Rosa², Emanuel Vitor Pereira Apolonio², Mariana Correa Rossi², Carlos Eduardo Fonseca-Alves², Carlos Alberto Hussni², Celso Antonio Rodrigues², Marcos Jun Watanabe², Anna Paula Balesdent Barreira^{2,3}, Ana Liz Garcia Alves^{2*}

Abstract

Synovial membrane-derived mesenchymal stem cells (_{SM}MSCs) demonstrate high chondrogenic potential in joint injuries, but their early dispersion decreases their immunomodulatory and reparative properties. This study aimed to evaluate the effect of encapsulated _{SM}MSCs in alginate hydrogels on induced chondral lesions in horses. Lesions were surgically induced in the talus of fifteen horses treated with PBS, free or encapsulated _{SM}MSCs from an allogeneic cell bank. Clinical, orthopedic and synovial analyses were performed at baseline and on Days 1, 2, 4, 7 and 14 for cytological and biomarker analyses (IL-1, IL-6, IL-10, PGE₂, TNF α , INF- γ , IGF, P Substance and SAA). At Day 150, cartilage biopsies were performed for macroscopic, histological and immunohistochemical analyses. The results were statistically significant when $p \leq 0.05$. Lameness and articular distention were observed in all horses on Days 1 and 2. There was an increase in TNCC and neutrophil count at Day 1 in all groups, which was significantly higher in the encapsulated _{SM}MSC group. This group also showed an earlier peak of macrophages and lymphocytes. There was no significant difference between groups on biomarker analysis but between time points for IL-1 α , IL-6, INF- γ and SAA in the cell groups. The encapsulated _{SM}MSC group also presented significantly higher Global Repair Evaluation, histological and immunohistochemical scores. Therefore, _{SM}MSCs encapsulated in alginate beads presented immunomodulatory capacity, resulting in intensified and premature inflammatory reactions and better macro- and microscopic aspects of tissue repair than the other groups, providing better outcomes for equine tarsus chondral lesions.

Keywords: Alginate; Bioengineering; Horses; Immunomodulation; Osteoarthritis

Abbreviations: _{SM}MSC: Synovial Membrane Mesenchymal Stem Cells; PBS: Phosphate Buffered Saline; IL- Interleukin; INF: Interferon; TNF: Tumor Necrosis Factor; TGF: Transforming Growth Factor; IGF: Insulin Growth Factor; PGE: Prostaglandin E; OA: Osteoarthritis; MSC: Mesenchymal Stem Cell; CaCl: Calcium Chloride; NaCl: Sodium Chloride; ICRS: International Cartilage Repair Society; IHC: Immunohistochemistry; DAB: 3,3'-Diaminobenzidine Tetrahydrochloride; TNC: Total Nucleated Cells; TP: Total Protein; SAA: Serum Amyloid A; SP: Substance P; NC: Nucleated Cells; MC: Macrophages Cells; LC: Lymphocytes Cells; GRE: Global Repair Evaluation; HE: Hematoxylin Eosin; COL II: Collagen Type II; PRP: Plasma Rich Platelets; LPS: Lipopolysaccharide.

Affiliation:

¹State University of Londrina (UEL), Highway Celso Garcia Cid KM 380, Londrina, Paraná, Brazil

²Department of Veterinary Surgery and Animal Reproduction, Regenerative Medicine Lab, School of Veterinary Medicine and Animal Science, São Paulo State University (UNESP), Botucatu, São Paulo, Brazil

³Department of Veterinary Medicine and Surgery, Veterinary Institute, Rural Federal University of Rio de Janeiro (UFRRJ), Seropedica, Rio de Janeiro, Brazil

*Corresponding Author:

Ana Liz Garcia Alves, Department of Veterinary Surgery and Animal Reproduction, Regenerative Medicine Lab, School of Veterinary Medicine and Animal Science, São Paulo State University (UNESP), Botucatu, São Paulo, Brazil.

Email: ana.liz@unesp.br

Citation: Vitor Hugo Santos, João Pedro Hübbe Pfeifer, Gustavo Santos Rosa, Emanuel Vitor Pereira Apolonio, Mariana Correa Rossi, Carlos Eduardo Fonseca-Alves, Carlos Alberto Hussni, Celso Antonio Rodrigues, Marcos Jun Watanabe, Anna Paula Balesdent Barreira, Ana Liz Garcia Alves. Synovial-Derived Mesenchymal Stem Cells Encapsulated in Alginate Beads Provide Better Outcomes for Equine Tarsus Chondral Lesions. *Journal of Orthopedics and Sports Medicine*. 5 (2023): 265-279.

Received: May 17, 2023

Accepted: May 24, 2023

Published: June 01, 2023

Introduction

Osteoarthritis (OA) is the main cause of lameness in horses, leading to poor performance and great economic impact [1]. Its pathogenic processes are related to irregular mechanical forces, damaging chondrocytes and releasing proteases that result in articular hyaline cartilage fibrillation [2,3]. Currently, there is no fully successful treatment for chondral lesions, so cell-based therapy and tissue engineering can help to promote better chondral healing, reduce fibrocartilage and increase functional recovery [4].

Therapeutic strategies combining Mesenchymal Stem Cells (MSCs) with biocompatible scaffolds and bioactive components could better contribute to joint repair. Collagen hydrogel patches and hyaline cartilage allografts are described as possible scaffolds, providing mechanical support to implanted stem cells [4,5], but a search has been made for new materials.

Alginate hydrogel is a polysaccharide that can be extracted from brown seaweed or produced by bacteria, such as *Pseudomonas* and *Azotobacter* [6]. Initially, it was used for drug encapsulation [7] and recently for enfolding living cells in humans, horses, rabbits and rats [8-12].

Although the use of many cell sources has demonstrated positive results, synovial membrane-derived mesenchymal stem cells (_{SM}MSCs) stand out due to their high proliferation capacity, superior chondrogenic potential and easy harvest [13-16]. Treatment of OA using MSCs relies on their immunomodulatory and paracrine effects, which result in decreased lymphocyte activation and release of several molecules and growth factors (IL-10, IL 1ra, TGF- β and PGE2) involved in the articular repair process [5,17-24].

Despite all the benefits that tissue engineering brings to orthopedics, some undesired events remain, such as systemic dispersion [25] and decreased cell viability after intra-articular injection. Thus, recent studies have used encapsulated stem cells in joint injury therapy aiming to protect the cells and maintain their viability and capacity for chondrogenic differentiation [26].

This study aimed to evaluate the effect of encapsulated _{SM}MSCs in alginate hydrogels on induced chondral lesions in horses, either in the early inflammatory phase or later in chondral healing.

Material and Methods

Ethical Approval

This study was carried out under approval of the Ethics Committee on Animal Use of the Faculty of Veterinary Medicine and Animal Science – FMVZ, UNESP (protocol n.032/2020), registered in the Brazilian National Council for Animal Control and Experimentation - CONCEA (CIAEP n. 01.0115.2014, 06/05/2014). This seal guarantees the project's

alignment with the precepts of Law 11,794 of October 8, 2008, with Decree 6,899 of July 15, 2009, as well as with the rules issued by the CONCEA.

Experimental Animals

Fifteen healthy crossbred horses, ranging from 3–8 years of age and with a mean weight of 330 kg, participated in this study. Inclusion criteria were no history of orthopedic issues, absence of lameness (AAEP scale), no signs of tibiotarsal joint diseases on physical and radiographic exams and baseline synovial fluid cytology < 500 nucleated cells/ μ L. The animals were kept at the FMVZ University Farm in a semi-intensive breeding system. They were fed with Tifton hay, commercial horse feed (1% of body weight) and Coast-cross grazing grass. Only one limb from each animal was used, randomly chosen to assign the experimental groups with five animals each: encapsulated _{SM}MSCs, free _{SM}MSCs and PBS control.

Study Design

Chondral lesions were surgically induced in the talus medial trochlea of fifteen horses. Animals were treated with PBS, free _{SM}MSCs or encapsulated _{SM}MSCs from an allogeneic cell bank. General clinical exams, lameness evaluation and synovial analysis were performed. Samples were collected at baseline and Days 1, 2, 4, 7 and 14 for cytological analysis and dosage of biomarkers. At Day 150, cartilage biopsies were surgically performed for macroscopic, histological and immunohistochemistry analysis (Figure 1).

Clinical Evaluation

General clinical and orthopedic exams were performed by two blinded evaluators (CBCV Diplomate - Brazilian College of Veterinary Surgery). At baseline, Days 1, 2, 4, 7 and 14, general clinical (rectal temperature, respiratory and cardiac rate, mucosal color and capillary refill time) and orthopedic (heat, pain, distention of tibiotarsal joint and lameness evaluation [27] in walk/trot on straight line with/without flexion) exams were performed.

Radiographic Evaluation

Radiographs of the tibiotarsal joint were performed at baseline as an inclusion criteria exam. A portable diagnostic X-ray unit, Poskon model VET-20BT (50-90kV/8-20mA), with a Canon digital plate was used. Lateromedial, dorsoplantar, dorsolateral-plantaromedial oblique, dorsomedial-plantarolateral oblique and flexed lateromedial views were captured, and images were stored in a digital system for evaluation by two blinded evaluators (ABRV Diplomate - Brazilian College of Veterinary Radiology). Animals were excluded if they presented radiographic signs of OA, such as sclerosis or lysis of subchondral bone, soft tissue thickening, joint space narrowing, presence of osteophytes, enthesophytes or intra-articular fragments.

Arthrocentesis

Tibiotarsal arthrocentesis was performed at all-time points from the medial pouch, 2 cm distal to the medial malleolus of the tibia and caudal to the saphenous vein, using a 30 mm × 21 gauge needle and a 5 mL syringe. Synovial fluid was collected in tubes with and without EDTA. Samples with EDTA were analyzed immediately after collection for protein concentration and cytological evaluation, while samples without EDTA were centrifuged at 760 g for 10 minutes at 4°C, and the supernatant was stored in a -80°C freezer for joint inflammatory biomarker analysis.

Synovial Fluid Evaluations

Cytological analysis consisted of Total Nucleated Cell Counts (TNCCs) in a Neubauer chamber and specific counts of neutrophils, macrophages, and lymphocytes in a smear slide using Diff-Quik staining. Total protein concentrations were measured by refractometry. Inflammatory biomarker analysis was based on commercial enzyme-linked immunosorbent assay (ELISA) kits for the analysis of IL-1 α , IL-6, IL-10, INF- γ , TNF α (Milliplex Map Kit, Equine cytokine EQCYTMAG-93K, EMD Millipore Corporation, Germany), Substance P (Horse Substance P, MyBiosource, USA), Serum Amyloid A (Horse SAA Elisa Kit – MyBiosource, USA), IGF (Horse IGF-1 Insulin-like growth factor MyBiosource, USA) and PGE2 (PGE2 Elabscience BIotechnology Inc, USA), following the manufacturer’s instructions. Absorbance was read at a wavelength of 450 nm.

Cell Harvest and Culture

All SMMSC allogeneic cells were harvested from a healthy 3-year-old male American Quarter Horse donor and processed as described previously [28]. In short, a synovial membrane sample was collected within arthroscopy by shaver in a closed filtration system, and cells were previously characterized and cryopreserved in a biobank of the Cell Therapy Laboratory from FMVZ, UNESP. The anesthetic protocol was composed of preanesthetic

medication (acepromazine 0.05 mg/kg, IM; xylazine 0.5 mg/kg, IV), induction (diazepam 0.15 mg/kg, IV; ketamine 2.2 mg/kg, IV) and maintenance (isoflurane vaporized in 100% oxygen). Fragments of the synovial membrane of both metatarsophalangeal joints were collected with Rongeur Ferris Smith tweezers and submitted to successive washes with DMEM Knockout®, mechanical separation by scalpel blade and enzyme digestion with collagenase type I solution (2 mg/mL) diluted in DMEM Knockout® medium (Dulbecco’s Modified Eagle’s Medium). The solution was homogenized at 37 °C and 5.0% CO₂ overnight. The same volume of DMEM knockout medium was added to 10% heated Fetal Bovine Serum (FBS) and centrifuged at 628 g for 10 min. The supernatant was removed, and the culture medium was added for further centrifugation. This procedure was repeated one more time, and SMMSCs were cultured in 75 cm² culture flasks at a concentration of 10 × 10⁴ cells/cm² using Knockout® DMEM culture medium with 10% FBS. The flasks were kept in an environment-controlled oven at 37 °C and 5.0% CO₂.

Cell Encapsulation

For this study, cells were obtained by random selection and cultured until 1×10⁷ SMMSCs were in the third passage (P3), according to the described protocol [5,28]. The cells were characterized by adherence in the culture plate and immunophenotypic characterization by flow cytometry. Chondrogenic, osteogenic and adipogenic differentiation capacity was verified, confirming multipotentiality. Cells express positive markers for CD44, CD90 and CD 105 and do not express MHC-II. Cells from the encapsulated SMMSC group were resuspended in 1.5% (w/v) sodium alginate. The mixture was dripped in a gelling solution of CaCl₂ 102 mM using a 10 ml syringe and a 21 G needle in an infusion pump. The drops were maintained within the solution for 10 minutes for the crosslinking reaction and capsule formation. Capsules were washed three times in 0.15 M NaCl before injection, and a final concentration of 1 × 10⁵ cells per capsule was

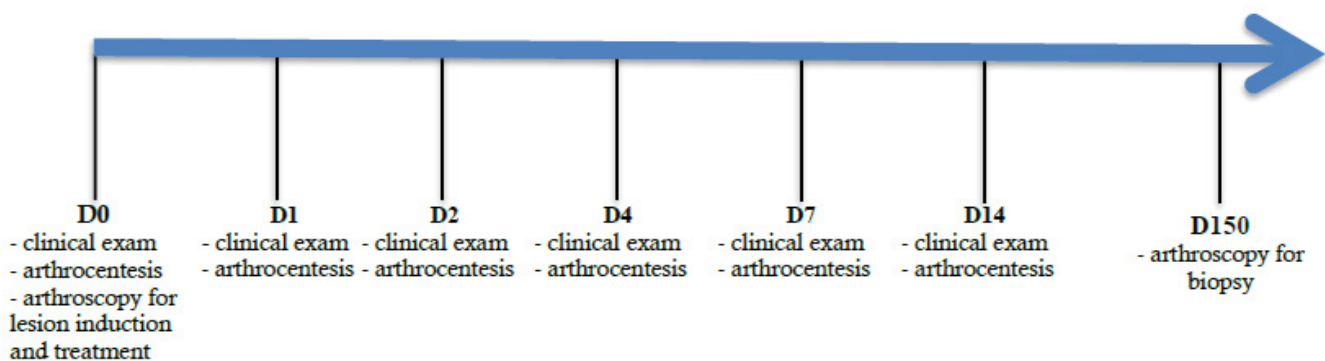


Figure 1: Study design from baseline (Day 0), when chondral lesions were surgically created at the medial trochlea talus bone and treatment was performed with 1×10⁷ encapsulated SMMSC cells (G1); 1×10⁷ SMMSC-free cells (G2) and 10 mL PBS for the control group (G3) until the end when biopsy was performed to allow for macroscopic, histological and immunohistochemistry analysis.

obtained, with a mean viability of 97,40%, as assessed by the Trypan Blue exclusion method in a Neubauer chamber. The entire cell preparation procedure was carried out within the laminar flow, ensuring an aseptic procedure.

Arthroscopic Procedure and Treatments

At the beginning of the experimental protocol, a chondral defect was induced in the middle third of the medial trochlea talus bone of fifteen tibiotarsals according to a previously described technique [29]. Briefly, a motorized shaver drill was used to create a 15 mm diameter and 1.5-3.2 mm depth chondral defect (Figure 2), and Ferris-Smith forceps were used to remove hyaline and calcified cartilage without reaching the subchondral bone.

All treatments were performed immediately after the induction of chondral defects in a volume of 10 ml ($_{SM}$ MSC-encapsulated 1×10^7 cells; $_{SM}$ MSC-free 1×10^7 cells and PBS control). The capsules were injected through the arthroscopic portal with a Levine catheter 20 mm in diameter. Animals received a single dose of dipyrone 25 mg/kg intravenously and an association of penicillins, with a dose calculated by benzathine (30,000 IU/kg, IM), every 72 h, 3 times. Additionally, daily dressing was performed with 0.5% chlorhexidine digluconate for 15 days after surgery until the stitches were removed.

A new arthroscopy procedure with a similar protocol was performed after 150 days to observe the macroscopic aspect of the chondral surface in situ and to collect a cartilage sample for histological analysis and immunohistochemistry.

Histological and immunohistochemistry Analysis

The cartilage aspect was graded according to the International Cartilage Repair Society (ICRS) score, which evaluates cartilage repair, lesion edge integration, macroscopic appearance and general aspect of the repair tissue. This grading was performed on recorded arthroscopy images by three blinded evaluators (Diplomate on CBCV - Brazilian College of Veterinary Pathology). Chondral tissue was harvested and cryopreserved using Tissue-Tek®

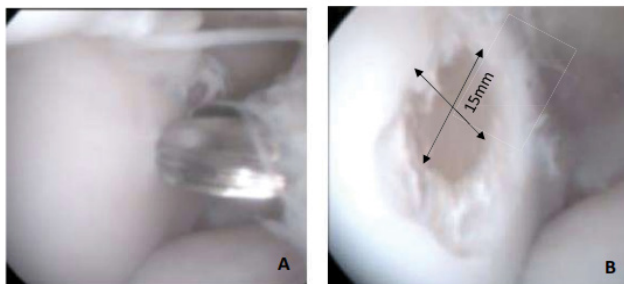


Figure 2: (A) Tibiotarsal arthroscopy (talus medial trochlea) before induced chondral lesion and (B) after chondral lesion performed at baseline (0 h).

O.C.T.™ compound (Sakura Finetek Europe B.V., Germany) for histological evaluation (hematoxylin-eosin and toluidine blue staining) according to the O'DRISCOLL histological score.

Immunohistochemistry (IHC) was performed according to a previously described technique based on the peroxidase and 3,3'-diaminobenzidine tetrahydrochloride (DAB) method. In short, antigen retrieval was performed using citrate buffer (pH 6) in a pressure cooker (Pascal®; Dako, Carpinteria, CA, USA) and the glass slides were placed into the autostainer Dako Cytomation (Pascal®; Dako, Carpinteria, CA, USA) platform. Anti-type II collagen antibody was detected using a mouse secondary monoclonal antibody (Sigma Aldrich, Saint Louis, Missouri, USA) at a 1/200 dilution. Immunologic staining was performed using Histofine (414154F, Nichirei Biosciences, Tokyo, JP), and the slides were counterstained with hematoxylin. The positive control was pulmonary tissue, whereas the negative control was made without primary antibody.

All samples were evaluated by bright field microscopy and graded in a semiquantitative scoring system, where the absence of expression was scored as 0; 1% to 25% positive staining was graded as 1; 26% to 50% positive staining was graded as 2 (weak); 51% to 75% positive staining was graded as 3 (moderate); and a score of 4 indicated that more than 75% of cells were stained (strong).

Statistical Analysis

A normality test was performed using the Kolmogorov-Smirnov test. In the absence of normality, the Kruskal-Wallis test was applied for comparisons between groups at the same time points, and the Friedman test was applied for comparisons between time points of each group. Tukey's test was performed for comparison between medians using Sigmatat 3.5 software when there was significance.

Data regarding treatment response were analyzed by general linear model ANOVA (GLM) considering the evaluator and the experimental group as constant. In the case of significance, mean values were compared by Tukey's test. Descriptive analysis is presented as the mean \pm SEM or proportion. A significant difference was considered when $p \leq 0.05$.

Results

Cell Viability

Just before treatment, the free $_{SM}$ MSC group demonstrated a mean count of 1.4×10^7 and 98,20% viability, whereas the encapsulated $_{SM}$ MSC group revealed a mean count of 1.5×10^7 and 97,40% viability. This treatment was composed of approximately 150 beads with approximately 1×10^5 cells each (Figure 3).

Clinical Exam

Injection of SMMSCs or PBS caused no adverse effects. The systemic physical parameters did not vary at any time point, remaining within the physiological range for the species. Selected joints developed mild to moderate synovial effusion and grade 2 lameness at Days 1-2 but returned gradually to normal parameters at Day 7.

Synovial Fluid Results

The total nucleated cell count showed a significant increase at Day 1 in all experimental groups, with a statistically higher count in the encapsulated SMMSC group than in the other groups (p=0.047). Although total protein also showed higher concentration at Day 1 in all groups, there was statistical significance within time points only for cell groups (encapsulated p ≤ 0.001 and free p = 0.002), but with no difference between groups (Figure 4).

At the differential count, neutrophils presented a significant increase at Day 1 in all experimental groups, with a significantly higher count in the encapsulated SMMSC group than in the other groups (p=0.013). The peak counts of macrophages and lymphocytes were different between groups in the free SMMSC group (Day 2) compared to the other groups (Day 1), showing a chemotaxis delay of these cells in the free SMMSC group. There was also a significant reduction in the macrophage count of the cell groups at Day 4 compared to that of the PBS control group (Figure 5).

There was no significant difference between groups for any protein biomarker at any time point, despite some difference between time points for cell groups (Figure 6 and 7).

Interleukin concentrations indicated different patterns among groups, with significant differences only between time points in IL-1α for the encapsulated SMMSC group and IL-6 for both cell groups, which showed higher concentrations at Day 4, later than the PBS control group (Figure 6). Despite no significant difference, the IL-10 concentration indicated an earlier and higher peak of encapsulated SMMSCs (Day 1) when compared to other groups.

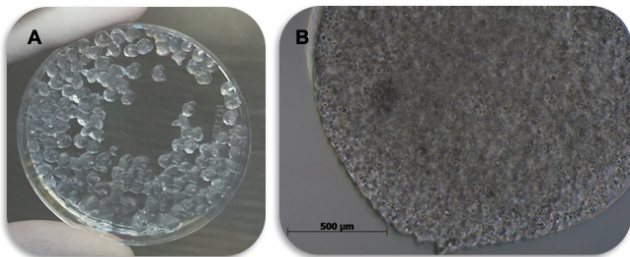


Figure 3: Equine synovial encapsulated membrane-derived mesenchymal stem cells in 1.5% sodium alginate hydrogel. (A) Capsules after gelification; (B) Bright field microscopy (20× objective lens) showing cell density, viewed as small beads.

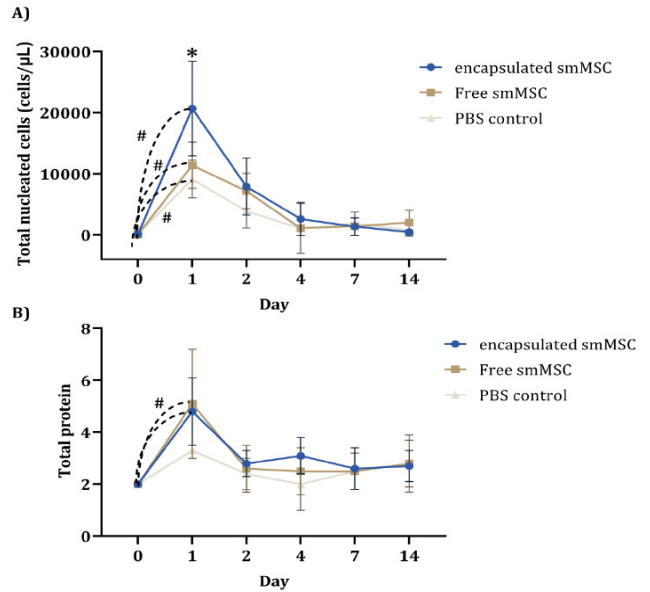


Figure 4: Mean cytology and biochemistry values of synovial fluid from the three groups over experimental time points: total nucleated cell count - TNCC (cells/μL) and total protein - TP (g/dL). There was a significant difference in both parameters (TNCC and TP) from Day 0 to Day 1 after lesion induction in the cell groups, free and encapsulated (p ≤ 0.05), indicating that the peak of acute inflammation was higher in the encapsulated SMMSC group than in the other groups.

Macroscopic Evaluation

Cartilage samples collected 150 days after treatment showed different macroscopic appearances among groups: the encapsulated SMMSC group demonstrated repair tissue similar to normal hyaline cartilage, free SMMSCs showed an incongruous cartilage surface joint, and the PBS control group still had erosive, irregular lesions, with filling failures, chondral defects and fibrosis with unfilled, friable and eroded areas. No signs of synovitis, fibrillation or erosion were observed in either cell group (Figure 9).

Global Repair Evaluation (GRE) showed significantly higher scores for encapsulated SMMSCs than for the PBS control. The results of all groups are presented in Table 1.

Histological and Immunohistochemical [SEP] Results

Histological analysis indicated different degrees of fibrocartilage deposition. However, while the PBS control group presented only fibrosis and fibrocartilage with no chondrocytes or extracellular glycosaminoglycan matrix, the encapsulated and free SMMSC groups demonstrated better tissue organization, visible chondrocytes and extracellular matrix deposition (Figure 10).

Immunohistochemistry for collagen type II did not present significant differences between groups, even though encapsulated and free SMMSC treatments showed higher

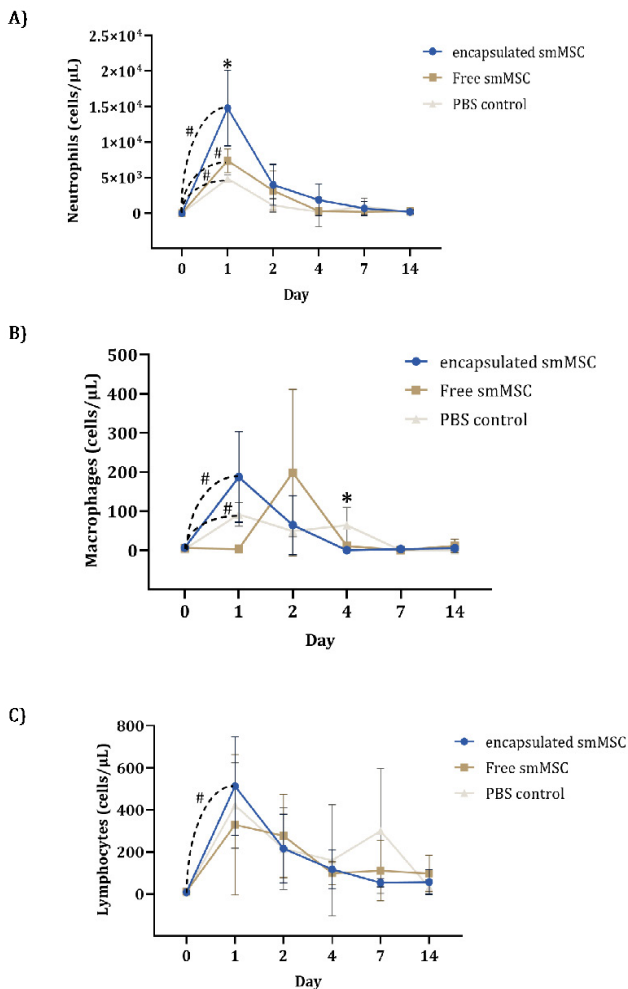


Figure 5: Cytology of synovial fluid of the groups over experimental time points: mean differential count of neutrophils, lymphocytes and macrophages (cells/µL). Asterisks indicate significant differences between groups at one time point ($p \leq 0.05$) and hashtags between time points.

labeling scores (4 and 3, respectively), in contrast to the score of 2 in the PBS control (Figure 10).

Histological scoring of O'DRISCOLL revealed significant differences between groups in structural integrity, chondrocyte grouping and lateral integration of the tissue (Table 2).

Discussion

The maintenance of systemic physiological parameters for two weeks after MSC injection reinforces the biosafety of this treatment, in agreement with previous studies [10,30].

Transitory lameness was described, associated with autologous, allogeneic and xenogeneic bone marrow MSCs [10,31] or allogeneic synovial-derived membrane MSCs [11], although the absence of lameness was also described in autologous bone marrow MSC injection of normal

equine joints [32]. In the present study, grade 2 lameness was observed in all horses at Day 1 and gradually returned to soundness at Day 7. Lameness was associated with joint distention, showing similar findings to previous studies from this research group [11]. We hypothesized that joint distention could result from the arthroscopy procedure for creating chondral lesions, a subsequent cascade of inflammatory events and capsule innervation compression, resulting in lameness, as described previously [5].

Cell characterization is a fundamental step for reliability and comparison of trials. Our results were similar to others,

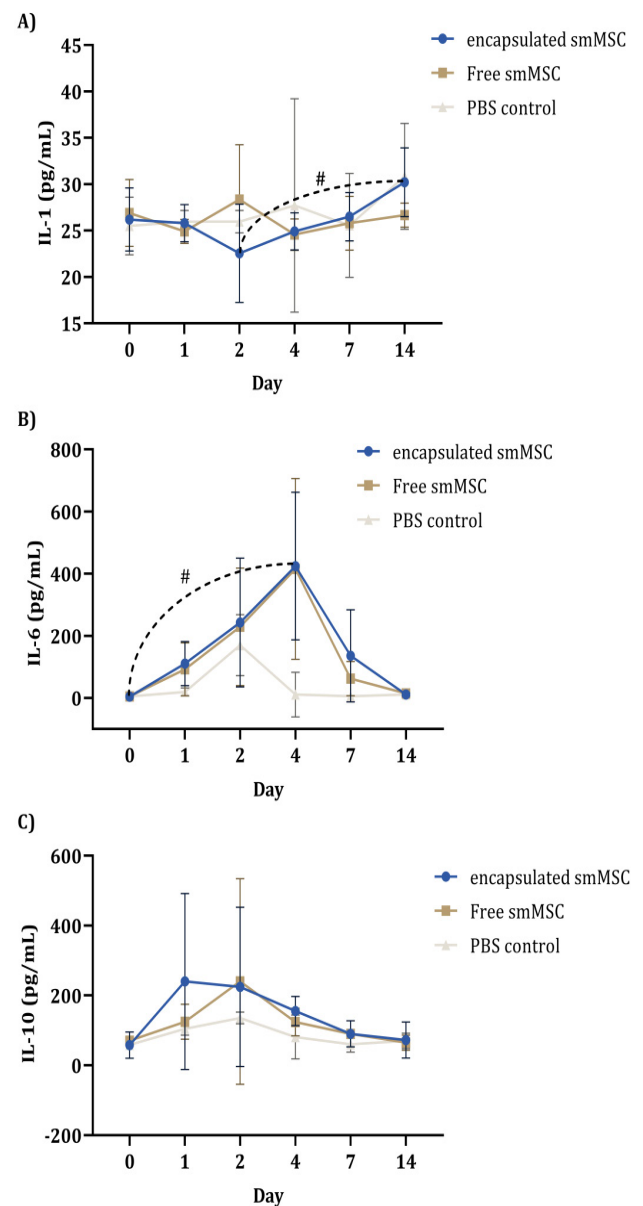


Figure 6: Mean concentration (pg/ml – y-axis) of IL-1 α , IL-6 and IL-10 in equine synovial fluid from experimental groups over time points (x-axis). Hashtags indicate significant differences between time points in the group ($p \leq 0.05$).

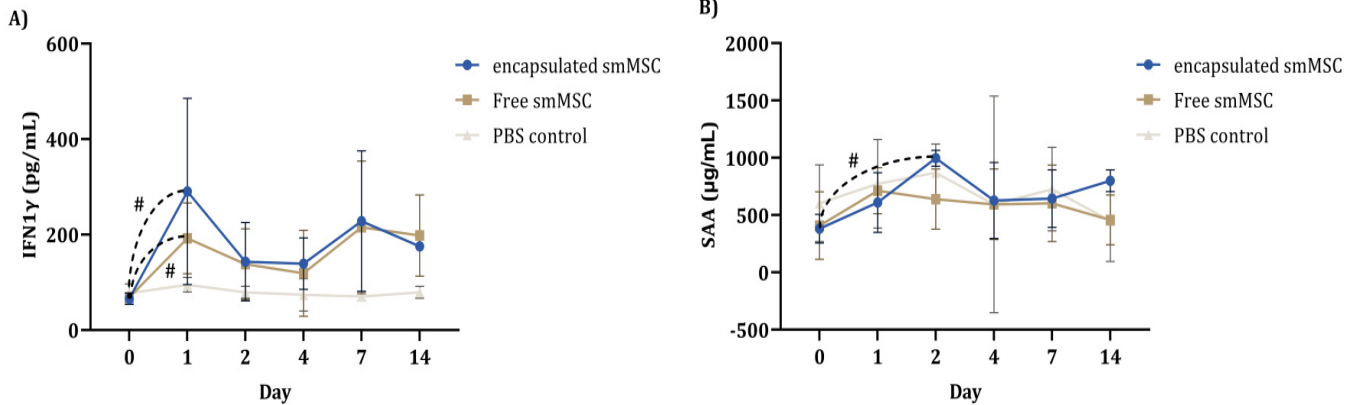


Figure 7: Mean concentration (pg/ml – y-axis) of IFN γ and SAA in equine synovial fluid from experimental groups over time points (x-axis). These were the only measured proteins that showed differences between time points (hashtag indicates $p \leq 0.05$), despite no difference between groups.

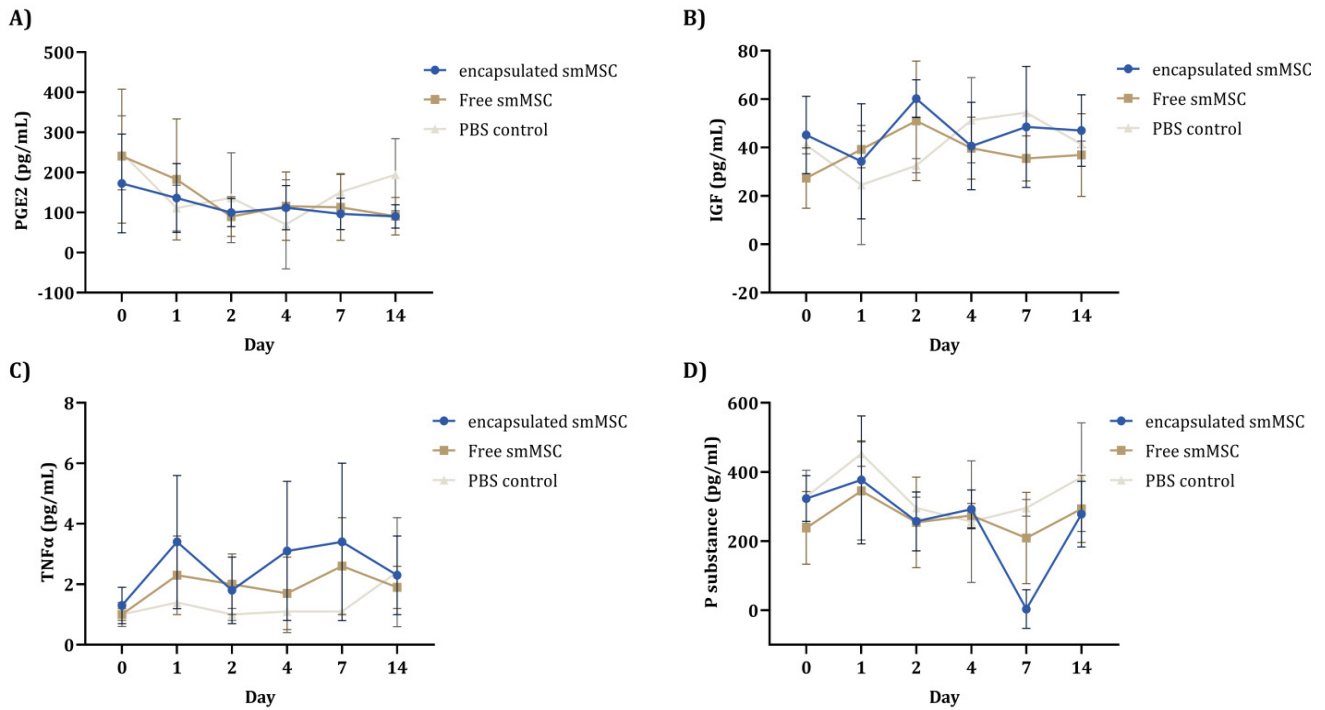


Figure 8: Mean concentrations (pg/ml – y-axis) of PGE2, IGF, TNF and P in equine synovial fluid from experimental groups over time points (x-axis) that did not demonstrate differences between time points or groups.

as SMMSCs presented adherence to plastic, chondrogenic, osteogenic and adipogenic differentiation, expression of CD44, CD90 and CD105 markers (TSAI, 2014) and did not express MHC-II [33,34].

The effects of MSCs in joint disorders have been evaluated in many studies, but questions about cell dispersion remain. It has been described that only 0.05% of cells remained in the joint 7 days after cell injection [24,35-37]. To try to reduce cell dispersion, there are studies on activated platelet-rich plasma (PRP) and different

kinds of scaffolds [8,38]. In our experimental conditions, SMMSCs maintained high viability and concentration after encapsulation in alginate hydrogel (1.5×10^7 and 97,40%), showing the recommended therapeutic cell concentration ($1-3 \times 10^7$) after the procedure [39].

An increase in total protein (TP) up to 5 g/dL was observed in both cell groups (encapsulated and free) at Day 1, in agreement with what has been demonstrated after allogeneic and xenogeneic MSC injections and indicates local inflammation [10].

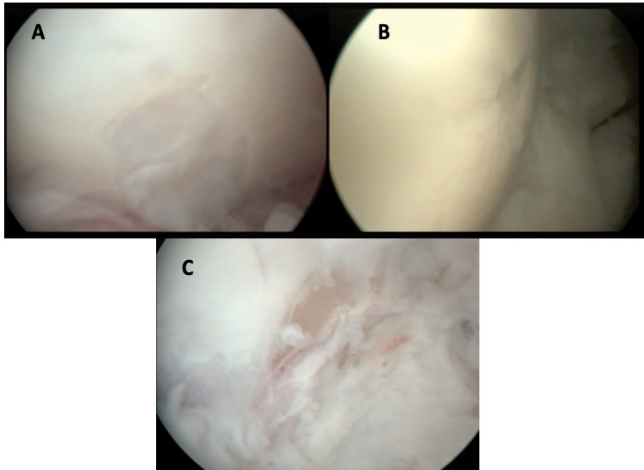


Figure 9: Results of macroscopic evaluation performed at Day 150. (A) The encapsulated SMMSC group showed total filling of the lesion by the neo-formed tissue similar to hyaline cartilage. (B) The free SMMSC group still exhibited chondral erosions and peripheral detachments. (C) The PBS control exhibited fibrosis, erosion and friable, poorly attached tissue.

Table 1: ANOVA for comparing group scores at Day 150 regarding “Global Assessment of Repair” (GRE).

Global Repair Evaluation (GRE)					
Group	Average	Standard Error	Standard deviation	Median	P
SMMSC free	8.6	0.4	0.894	8	0.007*
SMMSC encapsulated	10	0.707	1.581	10	
PBS control	6.6	0.245	0.548	7	

*Significant difference between groups.

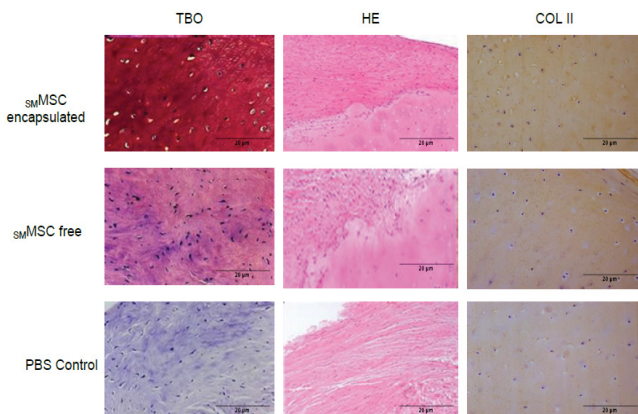


Figure 10: Microscopy bright field obtained at Day 150. Tissue was stained with HE, toluidine blue and immunohistochemistry for collagen type II (COL II). Encapsulated and free SMMSC treatments revealed better structural organization and the presence of chondrocytes and extracellular matrix.

In this study, it was hypothesized that the encapsulated SMMSC group would present a delay in the initial phases of the inflammatory process due to the gradual bioavailability that the scaffold should provide; however, this was not confirmed, as seen in the significantly higher peaks of neutrophils and macrophages in this group at Day 1. Although alginate itself is considered an inert biomaterial, the calcium used in the crosslinking process could exert an immunogenic effect [40]. In agreement, a trial demonstrated that alginate capsules injected into the mouse peritoneal cavity caused a significant increase in inflammatory cells at Days 2, 4 and 7 postinjection [41]. The present study did not investigate a group with alginate alone (without MSCs), which can be considered a limitation of this trial and should be done in further studies to evaluate the effect of alginate capsules alone (1.5% sodium alginate) without the MSC immunomodulatory paracrine effect.

Understanding macrophage concentration fluctuation in inflammation scenarios can be challenging because there are two antagonist phenotypes, M1 (proinflammatory) and M2 (anti-inflammatory), depending on the environment [42,43]. However, there was an increase in macrophage concentration at the initial time point in all groups (Days 1–2), with higher and earlier expression in the encapsulated SMMSC group than in the other groups. It is supposed that MSCs associated with alginate hydrogels could cause anticipation of the immune reaction. Based on studies associating the presence of M2 macrophages with the release of chondrogenic factors, including IL-10, IL-1Ra and TGF β [42,43], we suggested the predominance of M2 macrophages in encapsulated SMMSCs, mainly considering the coincidence peak of IL-10 at Day 1.

Lymphocytes are specialized cells of the adaptive or acquired immune system that are important for chronic inflammation and are responsible for recognizing and combating specific antigens [44]. In the present study, the significant increase in lymphocyte count at Day 1 in both cellular groups may have occurred due to the ability of MSCs to reduce lymphocyte activation, as described before [19,45], or to alginate hydrogel porosity that could result in transitory block antibodies and T cells [46].

In our study, regarding the analysis of inflammatory proteins, there was no significant difference between groups, which could be justified by differences in age, sex and variability in the method of OA induction when compared to other studies or by the complexity of the inflammatory cascade of in vivo protocols [47]. However, IL-1, IL-6, IFN1γ and SAA presented significant differences between time points.

IL-1 analysis can be challenging, as studies indicate concentrations below detectable limits in horses (0.02 pg/mL), showing results only in a few normal or inflamed

Table 2: Values resulting from histological scores of O'DRISCOLL (average, standard error, standard deviation, median and p value), ANOVA and Tukey's test for comparison between groups at Day 150.

	Group	Average	Standard error	Standard deviation	Median	P value
Tissue morphology	free _{SM} MSC	2.833	0.167	0.408	3	0.071
	encapsulated _{SM} MSC	2.167	0.307	0.753	2	
	PBS control	1.667	0.333	0.816	1.5	
Coloring matrix	free _{SM} MSC	2.5	0.224	0.548	2.5	0.59
	encapsulated _{SM} MSC	2.333	0.211	0.516	2	
	PBS control	2.167	0.167	0.408	2	
Structural integrity	free _{SM} MSC	3.333	0.333	0.816	3.5	0.028*
	encapsulated _{SM} MSC	2.333	0.211	0.516	2	
	PBS control	2.167	0.167	0.408	2	
Chondrocyte clustering at the implant site	free _{SM} MSC	2.667	0.211	0.516	3	0.013*
	encapsulated _{SM} MSC	3	0	0	3	
	PBS control	3	0	0	3	
Histological surface evaluation	free _{SM} MSC	2.833	0.167	0.408	3	0.149
	encapsulated _{SM} MSC	2.333	0.333	0.816	2.5	
	PBS control	2	0.258	0.632	2	
Lateral integration of the implanted material	free _{SM} MSC	2.667	0.211	0.516	3	0.031*
	encapsulated _{SM} MSC	2.5	0.224	0.548	2.5	
	PBS control	1.833	0.307	0.753	2	
Inflammation	free _{SM} MSC	1.33	0.211	0.516	1	0.237
	encapsulated _{SM} MSC	1.167	0.167	0.408	1	
	PBS control	1	0	0	1	

*Significant difference between groups.

joints [31]. Although increased IL-1 α / β secreted by synovial macrophages has been related to cartilage degradation/calcification and subchondral bone resorption [47,48], in vivo controlled studies in mice strongly suggested that IL-1 is not a key mediator in the development of OA, as the deficiency of the adaptor molecule for IL-1R1 did not impact the severity of experimental OA [47,49]. In the present study, IL-1 α could be detected at low concentrations and showed a mild elevation in free_{SM}MSCs and a reduction in encapsulated_{SM}MSCs simultaneously at Day 2, reinforcing the gradual bioavailability that the scaffold should provide.

The role of IL-6 in horses is not completely understood, despite knowledge of its being context dependent, playing pro- or anti-inflammatory roles [47,50]. This cytokine is released in LPS-induced arthritis [51] and is associated with proinflammatory effects, such as a delay in lymphocyte and neutrophil apoptosis and a decrease in T-cell stimulation [52,53]. Since the peak of IL-6 occurred in the PBS control group at Day 2 and in the encapsulated and free_{SM}MSC groups at Day 4, along with a decrease in neutrophil and total nucleated cell counts, we infer that_{SM}MSCs could downregulate inflammation and that IL-6 plays a role in this [31,54,55].

In the present study, the peak IL-10 concentration was earlier in the encapsulated_{SM}MSC group (Day 1) than in the other groups (Day 2), which suggested that when properly stimulated, MSCs can gradually release cytokines and other anti-inflammatory molecules, such as IL-1ra, indolamine 2,3-dioxygenase, TGF- β and PGE2[5,17,37]. Thus, it is possible that encapsulated MSCs could release IL-10 at Day 1 in response to the simultaneously high concentration of inflammatory cells, especially regulatory macrophages, that could also release IL-10, as suggested previously [44].

Encapsulated_{SM}MSCs seem to lead to an immunomodulatory effect, with earlier peaks of macrophages, lymphocytes and IL-10, higher counts of total nucleated cells and neutrophils, and elevated TNF α , IGF and IFN γ concentrations. This increase in IFN γ and TNF α can be related to the proinflammatory environment once IFN γ activates macrophages and TNF α activates neutrophils. TNF α is also related to tissue repair, influencing cell proliferation, differentiation, death and production of extracellular matrix [56]. This could be possible because of the porous structure of alginate that allows oxygen, metabolite and nutrient diffusion [57], including the release of cytokines and growth factors from the MSC [58-60].

Additionally, macro- and microscopic aspects of chondral healing indicate a better outcome in cartilage conditions after encapsulating SMMSCs in 1.5% sodium alginate, but the exact mechanisms have not been completely elucidated. In agreement with previous studies, alginate encapsulation provides MSC tridimensional organization, improves the delivery mechanism, increases therapeutic effects due to maintenance for a longer time at the site of injection [61-64], facilitates cell-to-cell interaction, increases specific cytokine release [65] and stimulates cells into a proresolutive scenario [18,37,66-68].

A longer follow-up of the animals would provide considerable data regarding collagen type II deposition and morphological and histological scores. Since each MSC source has its own particularities that may lead to different behaviors even when facing the same conditions, the comparison of the synovial membrane to other MSC sources would also contribute to a better understanding of the events associated with chondral healing in horses.

Although the best results were observed in the encapsulated SMMSC group, mainly in the histological scores, we infer that this study still has some limitations, such as the absence of the alginate control group and the performance of a larger histopathological study, not only from the lesion area. Further studies should also explore the comparison of different sources of MSCs and longer follow-ups to better understand collagen type II expression and the relevance of cytokines in the equine joint inflammatory environment.

Conclusions

In our experimental conditions, encapsulated SMMSCs increased neutrophil chemotaxis and induced earlier release of macrophages and IL-10, in addition to higher concentrations of IFN γ and SAA, highlighting their immunomodulation capacity. The treatment of encapsulated SMMSCs also resulted in better macro- and microscopic aspects of tissue repair, with higher glycosaminoglycan deposition and superior O'Driscoll scores.

Therefore, SMMSCs encapsulated in alginate beads provide better outcomes for equine tarsus chondral lesions, such as intensification of inflammation in the early phase confirmed by cytology and better chondral healing in the late phase evaluated by macroscopic observation, histology and immunohistochemistry. These results can provide important information for the clinical use of MSCs in animal and human patients. However, further studies should verify whether related findings could be attributed to SMMSCs, alginate hydrogels or both to contribute to a full comprehension of this scaffold interaction in the equine joint environment.

Acknowledgments

We thank the São Paulo Research Foundation (FAPESP

grant number 2017/12815-0 and 2017/14460-4), the Coordination for the Improvement of Higher Education Personnel (CAPES) and the National Council for Scientific and Technological Development (CNPq) for funding this study.

Authors' contributions

VH conceived the study and participated in its design, execution and coordination, in addition to writing the manuscript. JP, FC, MC and EV conceived the study and participated in its design, execution, data collection and manuscript review. GS and AP conceived the study and participated in its design, execution, data collection and manuscript review. LV and TR participated in the study design and performed the statistical analysis. CE participated in the design of the study and performed histological and immunohistochemical analyses. AL conceived the study, coordinated the research and carried out the writing and revision of the manuscript. All authors read and approved the final manuscript.

Funding

The São Paulo Research Foundation (FAPESP grant number 2017/12815-0 and 2017/14460-4) provided financial assistance for carrying out the entire research project. The Coordination for the Improvement of Higher Education Personnel (CAPES) and the National Council for Scientific and Technological Development (CNPq) contributed to the assistance of authors with scholarships.

Availability of data and materials

The authors will not share the data due to the pioneering work in the equine species.

Declarations

Ethics Committee approval

All experimental procedures were carried out in accordance with the approved guidelines and regulations of the Ethics Committee of São Paulo State University (protocol n. 032/2020).

Consent for publication

Not applicable.

Competing interests

The authors declare that they have no competing interests.

Author details

¹University of Veterinary Medicine and Animal Science UNESP, District of Rubião Júnior, s/n, Botucatu, São Paulo, Brazil. ²University State Londrina (UEL), Highway

Celso Garcia Cid KM 380, Londrina, Paraná, Brazil.
*Correspondence: ana.liz@unesp.br

References

- Sutton S, Clutterbuck A, Harris P, et al. The contribution of the synovium, synovial derived inflammatory cytokines and neuropeptides to the pathogenesis of osteoarthritis. *Vet J* 179 (2009): 10-24.
- Alcaraz MJ, Megías J, García-Arnandis I, et al. New molecular targets for the treatment of osteoarthritis. *Biochemical Pharmacology* 80 (2010): 13-21.
- McIlwraith CW, Frisbie DD, Kawcak CE. The horse as a model of naturally occurring osteoarthritis. *Bone Joint Res* 1 (2012): 297-309.
- Madeira C, Santhagunam A, Salgueiro JB, et al. Advanced cell therapies for articular cartilage regeneration. *Trends Biotechnol* 33 (2015): 35-42.
- Yamada ALM, Carvalho A de M, Moroz A, et al. Mesenchymal stem cell enhances chondral defects healing in horses. *Stem Cell Discov* 03 (2013): 218-225.
- Remminghorst U, Rehm BHA. Bacterial alginates: from biosynthesis to applications. *Biotechnol Lett* 28 (2006): 1701-1712.
- Lim F, Sun A. Microencapsulated islets as bioartificial endocrine pancreas. *Science* 210 (1980): 908-910.
- He X, Liu Y, Yuan X, et al. Enhanced healing of rat calvarial defects with MSCs loaded on BMP-2 releasing chitosan/alginate/hydroxyapatite scaffolds. *PLoS One* 9 (2014): 1-9.
- Kisiday JD, Kopesky PW, Evans CH, et al. Evaluation of adult equine bone marrow- and adipose-derived progenitor cell chondrogenesis in hydrogel cultures. *Journal of Orthopaedic Research*, 26 (2008): 322-331.
- Pigott JH, Ishihara A, Wellman ML, et al. Inflammatory effects of autologous, genetically modified autologous, allogeneic, and xenogeneic mesenchymal stem cells after intra-articular injection in horses. *Vet Comp Orthop Traumatol*. 26 (2013): 453-460.
- Rosa G, Kriek AMT, Padula E, et al. Allogeneic synovial membrane-derived mesenchymal stem cells do not significantly affect initial inflammatory parameters in a LPS-induced acute synovitis model. *Res Vet Sci* 132 (2020): 485-491.
- Williams LB, Koenig JB, Black B, et al. Equine allogeneic umbilical cord blood derived mesenchymal stromal cells reduce synovial fluid nucleated cell count and induce mild self-limiting inflammation when evaluated in an LPS induced synovitis model. *Equine Vet J* 48 (2015): 619-625.
- Yoshimura H, Muneta T, Nimura A, et al. Comparison of rat mesenchymal stem cells derived from bone marrow, synovium, periosteum, adipose tissue, and muscle. *Cell Tissue Res* 327 (2007): 449-462.
- De Bari C, Dell'Accio F, Tylzanowski P, et al. Multipotent mesenchymal stem cells from adult human synovial membrane. *Arthritis Rheum* 44 (2001): 1928-1942.
- Sakaguchi Y, Sekiya I, Yagishita K, et al. Comparison of human stem cells derived from various mesenchymal tissues: Superiority of synovium as a cell source. *Arthritis Rheum* 52 (2005): 2521-2529.
- Lee JC, Min HJ, Park HJ, et al. Synovial membrane-derived mesenchymal stem cells supported by platelet-rich plasma can repair osteochondral defects in a rabbit model. *Arthrosc - J Arthrosc Relat Surg* 29 (2013): 1034-1046.
- Shi Y, Su J, Roberts AI, et al. How mesenchymal stem cells interact with tissue immune responses. *Trends Immunol [Internet]* 33 (2012): 136-143.
- Van Lent PLEM, van den Berg WB. Mesenchymal stem cell therapy in osteoarthritis: Advanced tissue repair or intervention with smouldering synovial activation? *Arthritis Res Ther* 15 (2013): 1-2.
- Nöth U, Steinert AF, Tuan RS. Technology Insight: Adult mesenchymal stem cells for osteoarthritis therapy. *Nature Clinical Practice Rheumatology*. 4 (2008): 371-80.
- Drengk A, Zapf A, Stürmer EK, et al. Influence of platelet-rich plasma on chondrogenic differentiation and proliferation of chondrocytes and mesenchymal stem cells. *Cells Tissues Organs* 189 (2009): 317-326.
- Coleman CM, Curtin C, Barry FP, et al. Mesenchymal stem cells and osteoarthritis: Remedy or accomplice? *Hum Gene Ther* 21 (2010): 1239-1250.
- Frisbie DD, Smith RKW. Clinical update on the use of mesenchymal stem cells in equine orthopaedics. *Equine Veterinary Journal* 42 (2010): 86-89.
- Frisbie DD, Stewart MC. Cell-based Therapies for Equine Joint Disease. *Veterinary Clinics of North America - Equine Practice* 27 (2011): 335-349.
- Santos VH, Pfeifer JPH, Souza JB, et al. Evaluation of alginate hydrogel encapsulated mesenchymal stem cell migration in horses. *Res Vet Sci* 124 (2019): 38-45.
- Ayral X. Injections in the treatment of osteoarthritis. *Best Pract Res Clin Rheumatol*. 15 (2001): 609-626.
- Capes-Davis; Freshney RI. *Freshney's Culture of Animal Cells: A Manual of Basic Technique and Specialized Applications*: 6th ed. Wiley-Blackwell, New Jersey (2011).

27. Stashak TD. Adams and Stashak's Lameness in Horses, 6th ed. Wiley-Blackwell publishing, Iowa, USA (2011).
28. Santos VH, Pfeifer JPH, de Souza JB, et al. Culture of mesenchymal stem cells derived from equine synovial membrane in alginate hydrogel microcapsules. *BMC Vet Res* 14 (2018): 1-10.
29. Yamada ALM, Alvarenga ML, Brandão JS, et al. Arcabouço de PRP-gel associado a células tronco mesenquimais: Uso em lesões condrais em modelo experimental equino. *Pesqui Vet Bras* 36 (2016): 461-467.
30. Boone L. Intra-articular administration of allogeneic equine bone derived mesenchymal stem cells. Athens, Georgia: University of Georgia (2013).
31. Menarim BC, Gillis KH, Oliver A, et al. Autologous bone marrow mononuclear cells modulate joint homeostasis in an equine in vivo model of synovitis. *FASEB Journal* 33: (2019): 14337-14353.
32. Ardanaz N, Vázquez FJ, Romero A, et al. Inflammatory response to the administration of mesenchymal stem cells in an equine experimental model: Effect of autologous, and single and repeat doses of pooled allogeneic cells in healthy joints. *BMC Vet Res* 1 (2016): 1-9.
33. Gutierrez-Fernandez M, Rodríguez-Frutos B, Ramos-Cejudo J, et al. Comparison between xenogeneic and allogeneic adipose mesenchymal stem cells in the treatment of acute cerebral infarct: Proof of concept in rats. *J Transl Med* 13 (2015): 1-10.
34. To K, Zhang B, Romain K, et al. Synovium-Derived Mesenchymal Stem Cell Transplantation in Cartilage Regeneration: A PRISMA Review of in vivo Studies. *Frontiers in Bioengineering and Biotechnology* 314 (2019): 1-14.
35. Horie M, Choi H, Lee RH, et al. Intra-articular injection of human mesenchymal stem cells (MSCs) promote rat meniscal regeneration by being activated to express Indian hedgehog that enhances expression of type II collagen. *Osteoarthr Cartil* 10 (2012): 1197-1207.
36. Ozeki N, Muneta T, Koga H, et al. Not single but periodic injections of synovial mesenchymal stem cells maintain viable cells in knees and inhibit osteoarthritis progression in rats. *Osteoarthr Cartil* 24 (2016): 1061-1070.
37. Ter Huurne M, Schelbergen R, Blattes R, et al. Antiinflammatory and chondroprotective effects of intraarticular injection of adipose-derived stem cells in experimental osteoarthritis. *Arthritis Rheum* 64 (2012): 3604-3613.
38. Khatab S, Leijts MJ, van Buul G, et al. MSC encapsulation in alginate microcapsules prolongs survival after intra-articular injection, a longitudinal in vivo cell and bead integrity tracking study. *Cell Biol Toxicol* 36 (2020): 553-570.
39. Wike MM, Nydam DV, Nixon AJ. Enhanced early chondrogenesis in articular defects following arthroscopic mesenchymal stem cell implantation in an equine model. *J Orthop Res* 25 (2007): 913-925.
40. Colbath AC, Dow SW, Hopkins LS, et al. Single and repeated intra-articular injections in the tarsocrural joint with allogeneic and autologous equine bone marrow-derived mesenchymal stem cells are safe, but did not reduce acute inflammation in an experimental interleukin-1 β model of synovitis. *Equine Vet J* 52 (2020): 601-612.
41. Robitaille R, Dusseault J, Henley N, et al. Inflammatory response to peritoneal implantation of alginate-poly-L-lysine microcapsules. *Biomaterials*. 26, (2005): 4119-4127.
42. Fernandes TL, Gomoll AH, Lattermann C, et al. Macrophage: A Potential Target on Cartilage Regeneration. *Front Immunol* 11 (2020): 1-9.
43. Davis MJ, Tsang TM, Qiu Y, et al. Macrophage M1/M2 polarization dynamically adapts to changes in cytokine microenvironments in *Cryptococcus neoformans* infection. *MBio* 4 (2013): 1-10.
44. Cruvinel W de M, Mesquita Júnior D, Araújo JAP, et al. Sistema imunitário: Parte I. Fundamentos da imunidade inata com ênfase nos mecanismos moleculares e celulares da resposta inflamatória. *Rev Bras Reumatol* 50 (2010): 434-461.
45. Vinatier C, Mrugala D, Jorgensen C, et al. Cartilage engineering: a crucial combination of cells, biomaterials and biofactors. *Trends Biotechnol* 27 (2009): 307-314.
46. Gasperini L, Mano JF, Reis RL. Natural polymers for the microencapsulation of cells. *J R Soc Interface* 11 (2014): 1-19.
47. Nasi S, Ea HK, So A, et al. Revisiting the Role of Interleukin-1 Pathway in Osteoarthritis: Interleukin-1 α and -1 β , and NLRP3 Inflammasome Are Not Involved in the Pathological Features of the Murine Meniscectomy Model of Osteoarthritis. *Front. Pharmacol* 8 (2017): 282.
48. Dwivedi A, More U, Sanjay D, et al. Pro-inflammatory biomarkers and cytokines in the various stages of osteoarthritis. *Journal of Pharmaceutical Negative Results* 14 (2023): 466-472.
49. Nasi S, Ea HK, Chobaz V, et al. Dispensable role of myeloid differentiation primary response gene 88 (MyD88) and MyD88-dependent toll-like receptors (TLRs) in a murine model of osteoarthritis. *Joint Bone Spine* 81 (2014): 320-324.

50. Smith JK. IL-6 and the dysregulation of immune, bone, muscle, and metabolic homeostasis during spaceflight. *npj Microgravity* 4 (2018): 1-8.
51. Hawkins DL, MacKay RJ, Gum GG, et al. Effects of intra-articularly administered endotoxin on clinical signs of disease and synovial fluid tumor necrosis factor, interleukin 6, and prostaglandin E2 values in horses. *Am J Vet Res* 54 (1993): 379-386.
52. Raffaghello L, Bianchi G, Bertolotto M, et al. Human Mesenchymal Stem Cells Inhibit Neutrophil Apoptosis: A Model for Neutrophil Preservation in the Bone Marrow Niche. *Stem Cells* 26 (2008): 151-162.
53. Iwamoto M, Kurachi M, Nakashima T, et al. Structure-activity relationship of alginate oligosaccharides in the induction of cytokine production from RAW264.7 cells. *FEBS Lett* 579 (2005): 4423-4429.
54. Venn G, Nietfeld JJ, Duits AJ, et al. Elevated synovial fluid levels of interleukin-6 and tumor necrosis factor associated with early experimental canine osteoarthritis. *Arthritis Rheum* 36 (1993): 819-826.
55. Wittenberg RH, Willburger RE, Kleemeyer KS, et al. In vitro release of prostaglandins and leukotrienes from synovial tissue, cartilage, and bone in degenerative joint diseases. *Arthritis Rheum* 36 (1993): 1444-1450.
56. Alberts B, Jhonson A, Lewis J, et al. *Biologia molecular da célula*. 6th ed. Artmed: Porto Alegre, Brazil (2017).
57. Sun J, Tan H. Alginate-based biomaterials for regenerative medicine applications. *Materials (Basel)* 6 (2013): 1285-1309.
58. da Silva Meirelles L, Fontes AM, Covas DT, et al. Mechanisms involved in the therapeutic properties of mesenchymal stem cells. *Cytokine and Growth Factor Reviews* 20 (2009): 419-427.
59. Desando G, Cavallo C, Sartoni F, et al. Intra-articular delivery of adipose derived stromal cells attenuates osteoarthritis progression in an experimental rabbit model. *Arthritis Res Ther* 15: (2013).
60. Kim YS, Choi YJ, Koh YG. Mesenchymal Stem Cell Implantation in Knee Osteoarthritis: An Assessment of the Factors Influencing Clinical Outcomes. *Am J Sports Med* 43 (2015): 2293-2301.
61. Barminko J, Kim JH, Otsuka S, et al. Encapsulated mesenchymal stromal cells for in vivo transplantation. *Biotechnol Bioeng*. 108 (2011): 2747-2758.
62. Le Blanc K, Ringdén O. Immunomodulation by mesenchymal stem cells and clinical experience. *Journal of Internal Medicine* 262 (2007): 509-525.
63. Satué M, Schüler C, Ginner N, et al. Intra-articularly injected mesenchymal stem cells promote cartilage regeneration, but do not permanently engraft in distant organs. *Sci Rep* 9 (2019): 1-10.
64. Zhang QZ, Su WR, Shi SH, et al. Human gingiva-derived mesenchymal stem cells elicit polarization of M2 macrophages and enhance cutaneous wound healing. *Stem Cells* 28 (2010): 1856-1868.
65. Kim J, Hematti P. Mesenchymal stem cell-educated macrophages: A novel type of alternatively activated macrophages. *Exp Hematol* 37 (2009): 1445-1453.
66. Maggini J, Mirkin G, Bognanni I, et al. Mouse bone marrow-derived mesenchymal stromal cells turn activated macrophages into a regulatory-like profile. *PLoS One* 5 (2010): 1-13.
67. Tsai S-Y. Intra-articular transplantation of porcine adipose-derived stem cells for the treatment of canine osteoarthritis: A pilot study. *World J Transplant* 4 (2014): 196-205.

Data set

parameter	time points group	0	1	2	4	7	14	p value	time points
		mean ± standard deviation							
TOTAL NUCLEATED CELLS	PBS control	96.0 ± 36.8 A	9135.0 ± 3075.9 bB	3907.5 ± 2782.5 AB	1068.5 ± 4080.5 AB	1843.5 ± 1900.0 AB	758.5 ± 931.3 AB	0.044*	
	encapsulated smMSC	113.4 ± 93.5 A	20700.0 ± 7726.6 aB	7925.0 ± 4652.2 C	2605.0 ± 2704.3 CA	1360.0 ± 1424.8 CA	434.0 ± 418.6 C	≤ 0.001*	
	free smMSC	93.8 ± 61.2 A	11395.0 ± 3774.8 bB	7190.0 ± 17212.6 AB	1087.4 ± 489.8 AB	1419.0 ± 783.1 AB	2040.0 ± 1995.8 AB	0.021*	
	<i>p value - groups</i>	0.912	0.047*	0.549	0.406	0.840	0.252		
NEUTROPHILS	PBS control	0 A	4863.5 ± 480.1 bB	1095.0 ± 944.7 A	161.0 ± 2063.5 A	921.5 ± 1175.9 A	158.5 ± 217.1 A	0.007*	
	encapsulated smMSC	4.2 ± 7.3 A	14802.0 ± 5328.5 aB	3994.4 ± 2885.6 A	1858.0 ± 2212.6 A	666.6 ± 974.8 A	204.0 ± 292.0 A	≤ 0.001*	
	free smMSC	3.4 ± 6.1 A	7380.4 ± 1665.4 bB	3177.6 ± 9728.7 AB	286.6 ± 133.3 AB	204.0 ± 455.3 AB	291.8 ± 1607.4 AB	0.024*	
	<i>p value - groups</i>	0.732	0.013*	0.646	0.232	0.645	0.495		
MACROPHAGES	PBS control	3.0 ± 4.2 AC	91.5 ± 30.4 B	49.0 ± 14.1 ABC	64.0 ± 46.2 bAB	0 C	0 C	0.005*	
	encapsulated smMSC	6.4 ± 7.5 A	187.0 ± 115.4 B	64.4 ± 74.9 A	0 aA	3.2 ± 4.4 A	5.4 ± 5.8 A	≤ 0.001*	
	free smMSC	5.8 ± 6.0	3.4 ± 7.6	198.4 ± 212.2	11.2 ± 10.4 a	0	11.4 ± 17.0	0.136	
	<i>p value - groups</i>	0.825	0.698	0.332	<0.001*	0.235	0.511		
LYMPHOCYTES	PBS control	8.5 ± 3.5	422.0 ± 203.6	215.5 ± 194.5	160.5 ± 264.9	300.0 ± 297.0	32.0 ± 35.4	0.359	
	encapsulated smMSC	9.0 ± 8.7 A	513.0 ± 234.0 B	216.0 ± 163.1 A	117.8 ± 91.5 A	54.4 ± 20.0 A	57.2 ± 58.3 A	≤ 0.001*	
	free smMSC	11.4 ± 10.9 A	330.0 ± 333.9 A	276.8 ± 198.6 AB	99.8 ± 54.4 AB	111.2 ± 142.6 B	98.2 ± 86.0 B	0.009*	
	<i>p value - groups</i>	0.898	0.604	0.463	0.0663	0.158	0.488		
TOTAL PROTEIN	PBS control	2.0 ± 0	3.3 ± 0.1	2.4 ± 0.6	2.0 ± 1.0	2.5 ± 0.7	2.8 ± 1.1	0.181	
	encapsulated smMSC	2.0 ± 0 A	4.8 ± 1.3 B	2.8 ± 0.5 A	3.1 ± 0.7 A	2.6 ± 0.8 A	2.7 ± 0.6 A	≤ 0.001*	
	free smMSC	2.0 ± 0 A	5.1 ± 2.1 B	2.6 ± 0.9 A	2.5 ± 0.9 A	2.5 ± 0.7 A	2.8 ± 0.9 A	0.002*	
	<i>p value - groups</i>	1000	0.451	0.790	0.236	0.994	0.951		

Asterisks indicate statistical difference ($p \leq 0.05$), small letters represent difference between groups in the moment and capital letters represent difference among time points in each group.

parameter	time points	0	1	2	4	7
	group	mean ± standard deviation				
IL-1	PBS control	25.5 ± 3.1	26.0 ± 1.2	26.0 ± 1.2	27.7 ± 11.5	25.6 ± 5.6
	encapsulated smMSC	26.2 ± 3.4 AB	25.8 ± 2.0 AB	22.5 ± 5.3 B	24.9 ± 2.0 AB	26.5 ± 2.6 AB
	free smMSC	26.9 ± 3.6	24.9 ± 1.3	28.4 ± 5.9	24.6 ± 1.7	25.8 ± 2.9
	<i>p value - groups</i>	0.882	0.638	0.522	0.151	0.917
IL-6	PBS control	4.4 ± 0.4	18.8 ± 13.0	169.60 ± 98.3	10.7 ± 72.0	5.3 ± 0.3
	encapsulated smMSC	4.0 ± 0.7 A	110.1 ± 71.0 A	142.5 ± 207.5 AE	424.2 ± 237.8 B	135.3 ± 148.1 A
	free smMSC	4.5 ± 1.3 A	91.9 ± 85.5 A	128.8 ± 189.1 AE	414.9 ± 291.1 B	61.9 ± 55.4 A
	<i>p value - groups</i>	0.787	0.374	0.899	0.164	0.330
IL-10	PBS control	58.3 ± 0	104.8 ± 18.4	135.7 ± 16.7	81.1 ± 62.9	60.2 ± 22.4
	encapsulated smMSC	58.0 ± 37.5	240.2 ± 252.1	224.6 ± 228.5	155.4 ± 41.8	90.3 ± 37.4
	free smMSC	70.6 ± 8.5	124.8 ± 50.0	240.0 ± 294.0	124.1 ± 39.2	89.7 ± 9.3
	<i>p value - groups</i>	0.716	0.506	0.879	0.119	0.394
PGE2	PBS control	249.0 ± 92.3	111.6 ± 57.6	136.8 ± 112.1	70.4 ± 111.0	151.1 ± 46.1
	encapsulated smMSC	172.5 ± 123.3	136.3 ± 86.3	99.8 ± 35.2	112.6 ± 55.9	96.6 ± 39.1
	free smMSC	240.5 ± 167.0	182.4 ± 151.0	89.8 ± 49.6	115.9 ± 85.4	112.8 ± 82.1
	<i>p value - groups</i>	0.706	0.728	0.609	0.720	0.599
IGF	PBS control	41.5 ± 3.6	24.5 ± 24.6	32.5 ± 2.9	51.3 ± 17.6	54.4 ± 1.4
	encapsulated smMSC	45.2 ± 16.0	34.3 ± 23.8	60.2 ± 7.8	40.6 ± 18.1	48.5 ± 25.9
	free smMSC	27.4 ± 12.5	39.2 ± 7.6	51.0 ± 24.7	39.7 ± 12.8	35.5 ± 9.3
	<i>p value - groups</i>	0.160	0.649	0.215	0.632	0.403
TNFα	PBS control	1.0 ± 0.4	1.4 ± 0.1	1.0 ± 0.2	1.1 ± 0.7	1.1 ± 0.0
	encapsulated smMSC	1.3 ± 0.6	3.4 ± 2.2	1.8 ± 1.1	3.1 ± 2.3	3.4 ± 2.6
	free smMSC	1.0 ± 0.2	2.3 ± 1.3	2.0 ± 1.0	1.7 ± 1.2	2.6 ± 1.6
	<i>p value - groups</i>	0.623	0.366	0.490	0.308	0.422
IFN1γ	PBS control	77.3 ± 19.7	94.9 ± 15.2	79.0 ± 12.4	73.7 ± 34.1	70.3 ± 9.7
	encapsulated smMSC	65.6 ± 11.8 A	290.7 ± 195.0 B	143.1 ± 82.2 AB	139.9 ± 54.3 AB	228.3 ± 147.1 AE
	free smMSC	68.2 ± 5.7 A	192.6 ± 74.1 B	138.4 ± 77.8 AB	119.2 ± 90.3 AB	215.1 ± 139.5 B
	<i>p value - groups</i>	0.466	0.264	0.588	0.552	0.387
P substance	PBS control	328.9 ± 77.4	453.7 ± 37.2	296.1 ± 31.0	256.7 ± 176.5	296.1 ± 24.8
	encapsulated smMSC	323.1 ± 66.7	377.1 ± 185.1	257.8 ± 85.4	292.8 ± 56.0	3.2 ± 56.0
	free smMSC	238.0 ± 105.2	345.3 ± 142.8	254.5 ± 131.7	274.2 ± 35.4	209.6 ± 132.4
	<i>p value - groups</i>	0.283	0.718	0.887	0.791	0.578
SAA	PBS control	604.5 ± 334.2	774.9 ± 386.8	871.9 ± 249.7	593.1 ± 945.6	727.7 ± 365.6
	encapsulated smMSC	381.9 ± 125.1 A	1010.8 ± 260.6 AE	997.9 ± 69.2 B	1228.8 ± 332.2 AE	544.7 ± 251.5 AE
	free smMSC	409.9 ± 295.5	713.13 ± 200.0	640.9 ± 262.0	594.1 ± 308.4	603.0 ± 333.5
	<i>p value - groups</i>	0.550	0.702	0.055	0.987	0.888

Asterisks indicate statistical difference ($p \leq 0.05$) and capital letters represent difference among time points in each group